

# HYBRID PULSED LASER DEPOSITION OF Ti-Cu-N TERNARY NITRIDE THIN FILMS

G.M. Matenoglou<sup>1</sup>, G.A. Evangelakis<sup>2</sup>, C. Kosmidis<sup>2</sup> and P. Patsalas<sup>1</sup>

<sup>1</sup>University of Ioannina, Department of Materials Science and Engineering, GR-45110, Ioannina, Greece

<sup>2</sup>University of Ioannina, Department of Physics, GR-45110, Ioannina, Greece

Received: January 22, 2007

**Abstract.** In this work we present the growth of Ti-Cu-N ternary films by a hybrid Pulsed Laser Deposition (PLD) process. In the configuration used, the metal source was a composite Ti-Cu target, which was ablated by a high-fluence Nd:YAG laser (2nd harmonic,  $\lambda=532$  nm) in a flowing  $N_2$ . The process was carried out in a homogeneous electric field with the substrate being at a negative DC potential (bias voltage  $V_b=-50$  V) with respect to the ablation target. Films with the typical gold-like appearance of TiN were grown at  $P_{N_2} \sim 10^{-1}$  Pa. The effects of  $P_{N_2}$  to the Metal/N ratio and Ti/Cu ratio into the films, as well as the crystal structure of the films were studied employing Auger Electron Spectroscopy (AES) and X-Ray Diffraction (XRD), respectively. The films were found to consist of nanocrystalline TiN and amorphous Cu. Cu did not crystallize even in the Cu-rich films. The N was found to be bonded exclusively with Ti.

## 1. INTRODUCTION

Research in hard and ductile materials, especially in thin-film form, for mechanical application is of great interest in recent years. The combination of one soft-ductile phase (e.g. a noble metal or graphite) and one hard phase (e.g. a nitride or diamond-like carbon) can lead to a successful synthesis of superhard films either in nanocomposite [1] or in multilayer [2,3] form. Due to the large variety of possible material combinations, the hardness enhancement in hard-soft material systems is of great importance.

Composite ternary nitrides are very promising materials in this field, as it has to do with their mechanical properties, durability and toughness [4]. Particularly, nitrides of the form TM-NM-N, where TM and NM stand for Transition Metal and Noble Metal respectively, can exhibit a tension to form two separate phases, a soft metallic one and a hard nitride; in some cases the NM is distributed in the grain boundary region around the nitride grains [5,6], similar behavior has been also observed in

TMN-Ni [7] and TMN-Si films [8]. This comes as a result of the very low miscibility between NM and N and the high heat of formation of NM-N phase. Moreover, the properties of such a material can be tailored based on the existing metal and nitride phases [9]. The nitride phases provide hardness and the metal phases improve ductility of the composite structure.

The Ti-Cu-N ternary system has been investigated to study the formation of nanocomposites with low Cu concentration for use in superhard coatings [1,10]. However, the role of Cu in higher concentrations, which may result to formation of intermetallic Ti-Cu compounds, has not yet received so much attention, although the Ti-Cu intermetallic are also hard materials with potential use in biomedical applications and dentistry [11]. According to our knowledge there is no study of films incorporating TiN and Cu in comparable concentrations.

Furthermore, in this study we investigate the growth of Ti-Cu-N ternary films grown by a hybrid Pulsed Laser Deposition (PLD) process, which

Corresponding author: P. Patsalas, e-mail: ppats@cc.uoi.gr

employs an external electric field during growth, as described previously [12]. Although PLD was used to grow pure TiN [13,14], up to date was not reported to be used to grow such ternary films. Instead magnetron sputtering is the most popular technique for this purpose [1,5-8,10].

In this work we present our preliminary results regarding the PLD of TiN-Cu composite films. The scope of this paper is twofold: from one hand to investigate the feasibility of growing such films by PLD and on the other hand to study the formed phases during Ti and Cu co-deposition in  $N_2$  ambient, for high Cu concentrations. For the chemical and structural analysis we employ Auger Electron Spectroscopy (AES) and Grazing Incidence X-Ray Diffraction (GIXRD). We present the effects of the  $N_2$  partial pressure  $P_{N_2}$  to the TiN/N ratio, Ti/Cu ratio into the films, as well as the crystal structure of the films. We determine the optimized conditions for TiN and TiN-Cu growth and we investigate the phases formed during PLD growth.

## 2. EXPERIMENTAL

The PLD experiments have been performed in a turbo-pumped, high-vacuum chamber (base pressure  $P_b < 5 \cdot 10^{-5}$  Pa) presented in detail elsewhere [12]. The chamber is equipped with a rotating 45 mm target (0.25 Hz clockwise) and a rotating 50 mm sample holder (0.25 Hz counter-clockwise). The target to substrate distance was fixed at  $35 \pm 2$  mm. The rotating target consisted of pure Ti and Cu (99.95%) plates covering 50% and 50% respectively of the target holder area. The Ti-Cu-N films were grown on commercial Si{001} crystal wafers by a high-fluence Nd:YAG laser (2nd harmonic,  $\lambda = 532$  nm) (Lambda-Physik, pulse duration 3 ns, repetition rate 10 Hz) in a flowing  $N_2$  (99.999 %) ambient. The Nitrogen flow was controlled by an electronic Mass Flow Control (MFC) system and was kept constant,  $\Phi_{N_2} = 50$  sccm, in all experiments; the chamber pressure was varied by using a gate valve in front of the pumping system.

The laser beam was focused using a lens (50 cm focal position) outside the vacuum chamber passing through a fused silica viewport. In all experiments the pulse energy was kept constant at 200 mJ. A constant deposition time of 20 min was used for all samples. The process was carried out in a homogeneous electric field with the substrate being at a negative DC potential (bias voltage,  $V_b = -50$  V) with respect to the ablation target. The partial pressure of the ablated Ti-Cu vapor was about  $1 \cdot 10^{-3}$  Pa, while the base pressure  $P_b$  was  $< 5 \cdot 10^{-5}$

Pa. The  $N_2$  partial pressure ( $P_{N_2}$ ) varied between  $1 \cdot 10^{-2}$  Pa and 40 Pa. Under these conditions there was no self-sustained plasma generation (even for the highest  $P_{N_2}$  case) due to the low value of  $V_b$ . However, laser-induced plasma generation was observed for a wide range of pressures during laser illumination.

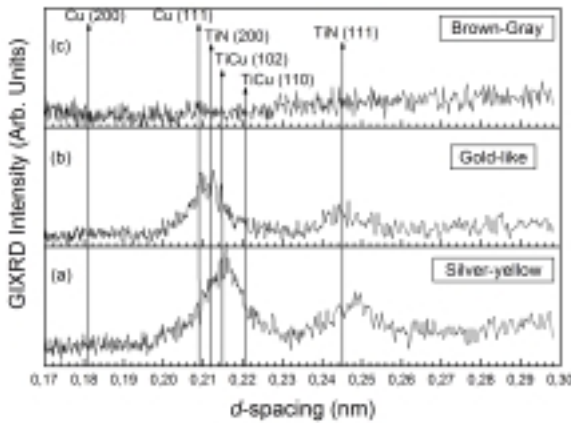
The produced Ti-Cu-N films were studied by Auger Electron Spectroscopy (AES), and X-Ray Diffraction (XRD). The AES spectra were acquired in a turbo-pumped ultra-high vacuum chamber ( $P_b < 5 \cdot 10^{-7}$  Pa), after bake-out at  $> 150$  °C for 36 h, using a concentric electron gun (3 KeV excitation energy) in a cylindrical mirror analyzer (CMA - Physical Electronics). XRD experiments were performed in Bragg-Brentano ( $\theta$ - $2\theta$ ) and grazing-incidence, asymmetric geometry using a monochromatized  $CuK_{\alpha}$  line and a line focus. For the grazing incidence XRD (GIXRD) experiments we used angle of incidence  $\alpha = 1^\circ$ , in order to be slightly bigger than the critical angle of these samples. X-Ray Reflectivity was also used to evaluate the film density and surface roughness.

## 3. RESULTS AND DISCUSSION

The hybrid PLD was employed to grow the Ti-Cu-N films with varying  $P_{N_2}$ . The process is hybrid because it combines the usual PLD with the addition of an external dc-electric field, which induces plasma generation during laser illumination. The produced plasma has a clear violet color, characteristic of  $N_2^+$  ions. Therefore, this process is more effective in creating nitride phases due to the activity of  $N_2^+$  compared to conventional PLD where the ablation occurs in pure  $N_2$  and the  $N_2^+$  species are only created by the laser and are not accelerated towards the substrate. The various  $P_{N_2}$  were used in order to identify the conditions to form the hard TiN phase in the films, as well as to investigate if there is a  $N_2$  pressure window where Ti-Cu intermetallics are formed. All the produced Ti-Cu-N films had the appearance of TiN with varying stoichiometry  $x = [N]/[Ti]$ , thus the films were light yellow/silver (as understoichiometric  $TiN_x$ ), gold-like (as TiN) and brownish-grey (as over-stoichiometric  $TiN_x$ ) [15]. The pressures used as well as a summary of the structural features and the colors of the grown films are summarised in Table 1. It is worth to note that no significant contribution of the red-like Cu in the color of the films was observed. This is attributed to the amorphous nature of the Cu phase as we will discuss below.

**Table 1.** The pressures used for the growth of Ti-Cu-N and the structural features and the appearance of the films.

Sample	$P_{N_2}$ (Pa)	Density (g/cm <sup>3</sup> )	Roughness (nm)	Grain Size (nm)	Lattice Size (nm)	Color
1	0.0050	6.2	3	9.6	0.430	Silver-Yellow
2	0.037	7.2	0	11.2	0.422	Gold-like
3	0.10	-	-	-	-	Gold-like
4	4.2	4.6	0.7	N/A	N/A	Brown-Gray
5	Sputtered, stoichiometric reference TiN					Gold-like

**Fig. 1.** GIXRD diffractograms from representative Ti-Cu-N films grown on Si by PLD. The vertical arrows indicate the characteristic  $d$ -spacings of the TiN, Cu and TiCu phases according to the JCPDS powder diffraction files [16].

Representative films (one silver-yellow, one gold-like and one brownish) were measured by XRD and GIXRD. The relative GIXRD diffractograms are presented in Fig. 1; the characteristic interplanar spacings ( $d$ -spacings) of the TiN, Cu and TiCu phases, according to the JCPDS powder diffraction files [16], are also indicated as vertical arrows. There is a clear deterioration of the crystalline quality of the films as we move from low (silver-yellow sample) to high (brown-grey sample)  $P_{N_2}$ ; the brown-grey sample did not exhibit any trace of crystallinity. In the case of the silver-yellow sample, two XRD peaks have been observed; the corresponding  $d$ -spacings are typical of TiN under compressive stress [17]. Although the one peak is close to the TiCu(102) line, the absence of the TiCu(110) strong line indicates that there are no TiCu inter-

metallics in crystalline form. We also do not observe any trace of crystalline Cu.

In the case of the gold-like film we observe that the shift disappears and the diffraction peaks coincide with the pattern of TiN. We would expect that this sample would be more stressed due to the higher  $P_{N_2}$  during growth and the higher density of this sample (see Table 1). Therefore, this behavior is attributed to the larger content of ductile Cu in the film, as we will show below, which may promote stress relief. The fine structure of the peak at  $d=0.21$  nm, which might be an indication of crystalline Cu, is comparable with the noise level and therefore cannot be used for Cu-phase identification. More detailed transmission electron microscopy observations and selective area electron diffraction patterns are required to identify the possible existence of crystalline Cu. Finally, for the highest  $P_{N_2}$  the film has a brown-grey color and it is in glassy state. The formation of only TiN crystalline grains explains why the color of the films is determined exclusively by the crystalline TiN<sub>x</sub> characteristics.

The mean size  $G$  of the TiN grains has been estimated by Scherrer's formula:

$$G = \frac{0.9 \cdot \lambda}{FWHM_{hkl} \cdot \cos \theta_{hkl}}, \quad (1)$$

where  $\lambda$  is the X-Ray wavelength and  $FWHM_{hkl}$  and  $\theta_{hkl}$  are the broadening and the bragg angle of either the (200) or (111) diffraction peak. For this analysis we used the (200) peak (as the strongest one) and for the determination of  $FWHM_{200}$  and  $\theta_{200}$  the experimental peaks were fitted by pseudo-Voigt curves. We should note here that the determined values by Scherrer's formula are only an estima-

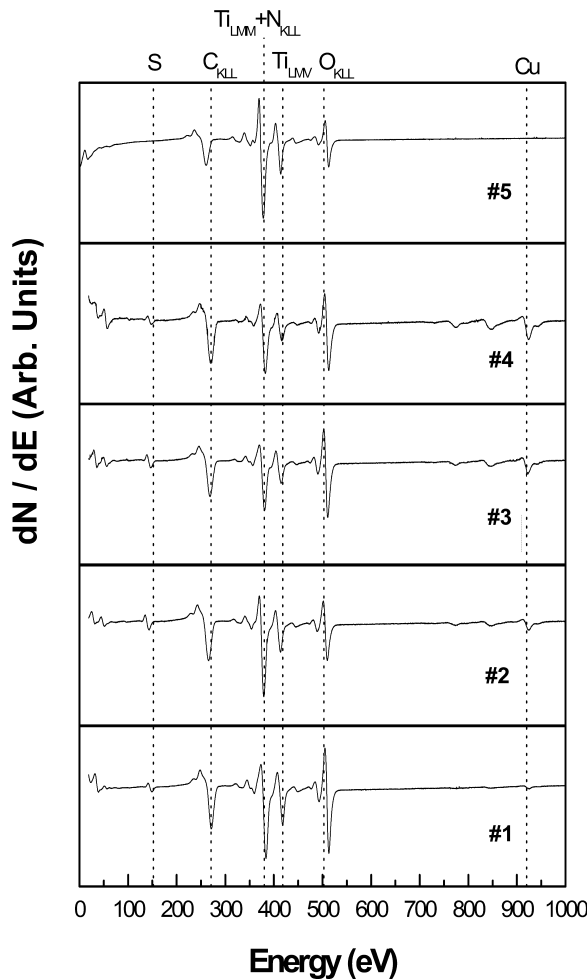


**Fig. 2.** The AES spectra of the samples of this study. The major AES peaks of Ti, N and Cu as well as those of the surface contaminations (O, C) are indicated by vertical dotted lines. The inset numbers correspond to the samples presented in Table 1.

tion and they are providing only the order of the grain size (nm or mm) because this kind of calculation may be severely affected by stress and strain effects. The  $G$  values summarized in Table 1 have been determined from the GIXRD data using the (200) peak. On the other hand, the  $G$  values determined from the Bragg-Brentano XRD scans are about 25% lower; this might be either due to the different diffraction geometry (the (200) diffracting grains are tilted by  $20^\circ$  between XRD and GIXRD experiments) or due to the high noise level in the conventional XRD experiments. Therefore, the

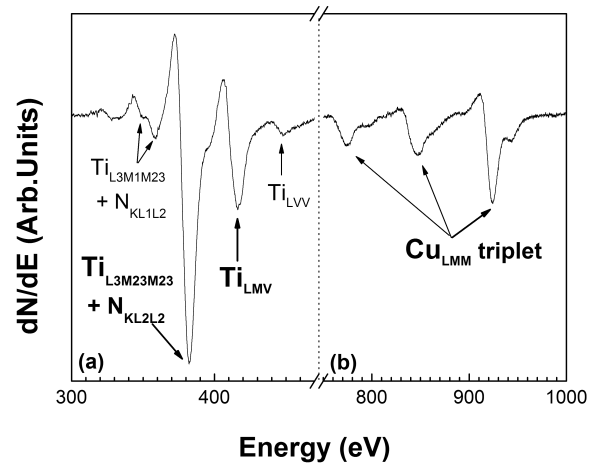


**Fig. 3.** Details from an AES spectrum (sample #4) showing the major (a) Ti, N, and (b) Cu lines and the relative assignments; bold letters and thick arrows indicate the lines used for the analysis.

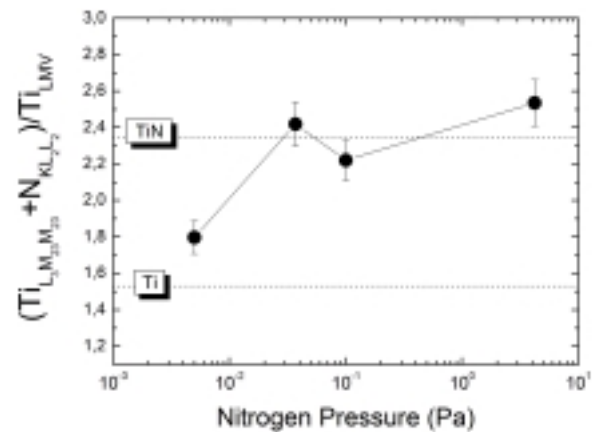


**Fig. 4.** The variation of the ratio of the  $Ti_{LMM}$  and  $N_{KLL}$  overlapping peaks over the  $Ti_{LMV}$  peak of Ti with the Nitrogen pressure during PLD. The horizontal lines indicate the values of this ratio for two reference samples of pure Ti and stoichiometric TiN.

XRD analysis indicate that the films consist of nanocrystalline TiN and amorphous metallic Cu phases.

The surface composition has been evaluated from the Auger spectra of the deposited films. The AES spectra are presented in Fig. 2 for all the studied samples; the AES data of a sputtered, stoichiometric, gold-like TiN reference sample, which was previously studied by X-ray Photoemission Spectroscopy and Ellipsometry. All the Ti-Cu-N films exhibit the characteristic AES peaks of Ti ( $Ti_{LMV}$  at 418 eV and  $Ti_{LVV}$  at 450 eV), the overlapped

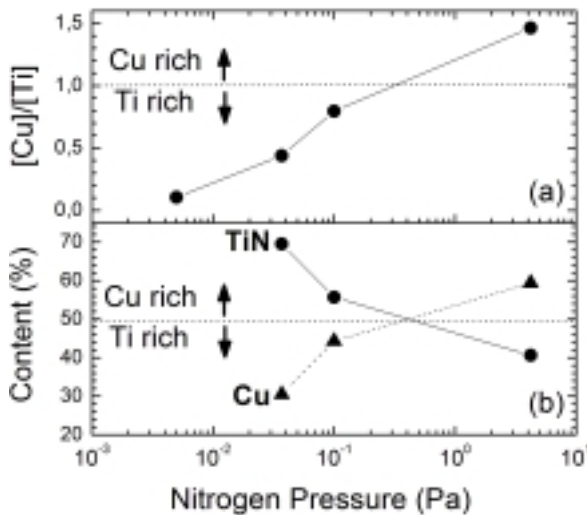


**Fig. 5.** (a) The variation of the  $[Cu]/[Ti]$  ratio with the working nitrogen pressure, and (b) the content of the TiN and Cu phases.

peaks of Ti with N ( $Ti_{L_{3M1M23}}/N_{K_{L1L2}}$  at 360 eV and  $Ti_{L_{3M23M23}}/N_{K_{L2L2}}$  at 380 eV) [18]. For simplicity in Fig. 2 the  $Ti_{L_{2M23M23}}$  and the  $N_{K_{L2L2}}$  lines are indicated as  $Ti_{LMM}$  and  $N_{KLL}$ , respectively. The characteristic  $Cu_{LMM}$  triplet between 780 and 920 [19], where the line at 920 eV is the strongest one, and the low kinetic energy peak ( $Cu_{M_{VV}}$  at around 60 eV [20]) of Cu have been also detected. We can also observe the  $O_{KLL}$  (503 eV) and  $C_{KLL}$  (271 eV) AES peaks, which originate exclusively from surface contamination due to exposure to lab atmosphere. This has been confirmed by Energy Dispersive X-Ray Spectroscopy (not shown here) in a Scanning Electron Microscope, which detected only traces of C and no O in the bulk of the films.

Measuring the relative heights of individual AES peaks we can evaluate the Ti, Cu and N content in the films. Fig. 3 shows details from the AES spectrum of sample #4 around the spectral region of the major Ti, N, and Cu lines and the relative assignments of the peaks. Bold letters and thick arrows are used to indicate the three lines ( $Ti_{L_{3M23M23}}/N_{K_{L2L2}}$ ,  $Ti_{L_{MV}}$  and  $Cu_{LMM}$ ) used for the following analysis. The  $[Cu]/[Ti]$  ratio has been determined quantitatively from the  $Ti_{L_{MV}}$  (418 eV) and the  $Cu_{LMM}$  (920 eV) lines, taking into account their sensitivity factors [21]. The quantification of the  $[N]/[Ti]$  ratio is not possible because of the overlap of the  $Ti_{L_{3M23M23}}$  and  $N_{K_{L2L2}}$  lines; however, a qualitative analysis based on the comparison of the relative strength of the ( $Ti_{L_{3M23M23}} + N_{K_{L2L2}}$ ) line and the

$Ti_{L_{MV}}$  line to the values of the two reference samples (pure Ti and stoichiometric TiN) has been carried out.

Fig. 4 shows the variation of the ratio of the  $Ti_{LMM}$  and  $N_{KLL}$  overlapping peaks over the  $Ti_{L_{MV}}$  peak of Ti with the Nitrogen pressure during PLD. The horizontal lines indicate the values of this ratio for two reference samples of pure Ti and stoichiometric TiN. For the lowest nitrogen pressure the ratio is closer to pure Ti, although the relative XRD pattern indicated that the only crystalline phase is TiN. Taking into account that we have not observed any trace of crystalline TiCu or Ti phases we may attribute this value of the ratio to under-stoichiometric  $TiN_x$  ( $x < 1$ ). This is also consistent with the color of this sample (pale silver-yellow). Increasing the content of  $N_2$  inside the chamber results to a raise in the  $[N]$  content in the nitride phase, where we obtain gold-like samples. The values of the ratio in Fig. 4 indicate the formation of stoichiometric TiN, in agreement to the XRD patterns. In this region, all of the Ti in the samples is consumed in forming TiN and thus no intermetallic phase can be formed. Combining the AES and XRD results we conclude that these gold-like films consist of pure nanocrystalline TiN and amorphous Cu phases. Further increase of  $P_{N_2}$  has a result to a ratio exceeding the value of TiN, meaning that all Ti is consumed to form TiN and there is additional excess of N. Taking into account that there is no indication for the  $Cu_3N$  phase in the XRDs and the color of the film is similar to over-stoichiometric  $TiN_x$  ( $x > 1$ ), this film is likely to consist of  $TiN_{x>1}$  and Cu.

Finally, the last structural/chemical feature, which was studied, is the relative concentrations  $[Ti]$  and  $[Cu]$ . Taking into account that Ti is completely consumed to form TiN (with the exception of sample #1) the  $[Cu]/[Ti]$  ratio might be used as a measure of the relative fractions of the TiN and Cu phases in the films. Fig. 5a shows the quantitative  $[Cu]/[Ti]$  ratios, determined from the  $Ti_{L_{MV}}$  and  $Cu_{LMM}$  lines taking into account their sensitivity factors [21], vs. the working nitrogen pressure. From this ratio the content of TiN and Cu phases in the films is determined (Fig. 5b) in the cases where Ti is completely consumed to form TiN. The increase of  $P_{N_2}$  promotes the incorporation of Cu in the film. The  $[Cu]$  increase with  $P_{N_2}$  affects also the XRD patterns (Fig. 1). Thus, the increase of ductile Cu absorbs the stress of the TiN phase causing the shift of the XRD lines towards the values of unstressed TiN. In addition, the increase of amorphous Cu reduces the diffracting volume of TiN grains result-

ing to weaker diffraction signal, as observed in Fig. 1b.

#### 4. CONCLUSIONS

A hybrid PLD process, which combines the conventional PLD with DC-plasma, was used to grow Ti-Cu-N ternary nitride films with high Cu content. The produced films consist of nanocrystalline TiN and amorphous Cu. No indication of formation of Ti-Cu intermetallic phases was observed, despite the high Cu content of the films; instead, Ti is consumed exclusively to form TiN in most cases. Various working nitrogen pressures were employed to vary the content of TiN and Cu phases as well as the stoichiometry of TiN. The color of the films is mainly affected by the TiN stoichiometry and no contribution from Cu was observed, due to the amorphous nature of Cu. Bright, gold-like films, with stoichiometric TiN grains are produced at  $P_{N_2} \sim 10^{-2}$  Pa.

#### ACKNOWLEDGEMENTS

This work is financially supported by the Greek Ministry of Education through the Grant: PYTHAGORAS II.

The Central Laser Facility of the University of Ioannina is acknowledged for providing the Laser source.

#### REFERENCES

- [1] J. Musil, P. Zeman, H. Hruby and P.H. Mayrhofer // *Surf. Coat. Technol.* **120–121** (1999) 179.
- [2] Y.Y. Tse, D. Babonneau, A. Michel and G. Abadias // *Surf. Coat. Technol.* **180–181** (2004) 470.
- [3] C. Mathioudakis, P. C. Kelires, Y. Panagiotatos, P. Patsalas, C. Charitidis and S. Logothetidis // *Phys. Rev. B* **65** (2002) 205203.
- [4] J.L. He, Y. Setsuhara, I. Shimizu and S. Miyake // *Surf. Coat. Technol.* **137** (2001) 38.
- [5] J. Musil and R. Daniel // *Surf. Coat. Technol.* **166** (2003) 243.
- [6] S. Veprek // *J. Vac. Sci. Technol. A* **17** (1999) 2401.
- [7] M. Benkahoul, C.S. Sandu, N. Tabet, M. Parlinska-Wojtan, A. Karimi and F. Levy // *Surf. Coat. Technol.* **188–189** (2004) 435.
- [8] A. Akbari, J. P. Riviere, C. Templier and E. Le Bourhis // *Surf. Coat. Technol.* **200** (2006) 6298.
- [9] Hyun S. Myung, Hyuk M. Lee, Leonid R. Shaginyan and Jeon G. Han // *Surf. Coat. Technol.* **163–164** (2003) 591.
- [10] K.P. Andreasen, T. Jensen, J.H. Petersen, J. Chevallier, J. Böttiger and N. Schell // *Surf. Coat. Technol.* **182** (2004) 268.
- [11] Masafumi Kikuchi, Yukyo Takada, Seigo Kiyosue, Masanobu Yoda, Margaret Woldu, Zhuo Cai, Osamu Okuno and Toru Okabe // *Dental Materials* **19** (2003) 174.
- [12] P. Patsalas, S. Kazianis, C. Kosmidis, D. Papadimitriou and G. Evangelakis // *J. Appl. Phys.*, submitted.
- [13] A. Giardini, V. Marotta, S. Orlando and G.P. Parisi // *Surf. Coat. Technol.* **151–152** (2002) 316.
- [14] B. Major, W. Mroz, T. Wierzchon, W. Waldhauser, J. Lackner and R. Ebner // *Surf. Coat. Technol.* **180–181** (2004) 580.
- [15] P. Patsalas and S. Logothetidis // *J. Appl. Phys.* **90** (2001) 4725.
- [16] JCPDS, *Powder Diffraction Files* : 38-1420 (TiN), 04-0836 (Cu), 65-2807 (TiCu).
- [17] P. Patsalas, C. Charitidis and S. Logothetidis // *Surf. Coat. Technol.* **125** (2000) 335.
- [18] R. Pantel, D. Levy and D. Nicolas // *J. Vac. Sci. Technol.* **A6** (1988) 2953.
- [19] J. Colino, J. L. Sacedon, L. Del Olmo and J. L. Vincent // *J. Vac. Sci. Technol.* **A8** (1990) 4021.
- [20] G. Chiarello, A. Amoddeo, R.G. Agostino, L.S. Caputi and E. Colavita // *Phys. Rev.* **B48** (1993) 7779.
- [21] L. E. Davis, N. C. MacDonald, P. W. Palmberg, G. E. Riach and R. E. Weber, *Handbook of Auger Electron Spectroscopy* (Physical Electronic Industries, Inc, Minnesota, 1978).